

**Damian WIERZBICKI<sup>1</sup>, Kamil KRASUSKI<sup>2,3</sup>**

<sup>1</sup>WOJSKOWA AKADEMIA TECHNICZNA, WYDZIAŁ INŻYNIERII ŁĄDOWEJ I GEODEZJI, 2 Sylwestra Kaliskiego Str., 00-908 Warsaw

<sup>2</sup>ZESPÓŁ TECHNIK SATELITARNYCH, 16 Zawiszy Czarnego Str., 08-530 Dęblin

<sup>3</sup>STAROSTWO POWIATOWE W RYKACH, WYDZIAŁ GEODEZJI, KARTOGRAFII I KATASTRU NIERUCHOMOŚCI, 10A Wyczółkowskiego Str., 08-500 Ryki

## Estimation of rotation angles based on GPS data from a UX5 Platform

### Abstract

Data integration from INS and GPS sensors is applied in aeronautical navigation as a basic conception for determination of aircraft position. A GPS sensor is used to estimate coordinates ( $X$ ,  $Y$ ,  $Z$ ) and velocity ( $V_x$ ,  $V_y$ ,  $V_z$ ) also in a navigation solution. On the other hand, an INS sensor provides rotation angles (heading, pitch and roll) and acceleration parameters ( $A_x$ ,  $A_y$ ,  $A_z$ ). The GPS sensor is preferred to obtain an approximate value of rotation angles. In this paper, the results of studies on determination of heading, pitch and roll angles using GPS technology are presented. For this purpose, GPS data from a single-frequency L1 receiver from a UX5 platform were used. Calculations were executed in the HPR\_GPS software, whose source code was written in Scilab 5.4.1 language. The software operation and an algorithm for estimation of heading, pitch, roll angles there is described. The preliminary results of rotation angles from the HPR\_GPS software show that heading, pitch and roll values are very similar to raw INS measurements. The mean difference between the GPS data (after Kalman filter operation) and the INS data for the heading angle is equal to  $0.32^\circ$  with a standard deviation of  $5.41^\circ$ , for the pitch angle is equal  $4.98^\circ$  with a standard deviation of  $5.06^\circ$  and for the roll angle is about  $0.06^\circ$  with a standard deviation of  $0.69^\circ$ .

**Keywords:** GPS, heading, pitch, roll, Kalman filter.

### 1. Introduction

The main conception of determining the aircraft position is based on satellite technology and inertial navigation in civil transport in the 21<sup>st</sup> century. In the case of the satellite technology, usually a GPS receiver is installed in an aircraft as a major sensor. This technique makes it possible to obtain the absolute position in the geocentric ( $X$ ,  $Y$ ,  $Z$ ) or geodetic ( $B$ ,  $L$ ,  $H$ ) frame and also a velocity component ( $V_x$ ,  $V_y$ ,  $V_z$ ). In the case of the INS approach, an IMU sensor offers rotation angles (heading, pitch and roll) and acceleration vectors ( $A_x$ ,  $A_y$ ,  $A_z$ ) [11]. Both sensors provide 6 parameters for calculation of the position in numerical processing. A part of GPS products (e. g. velocity components) can be utilized to determine approximate rotation angles, as an alternative technique relative to INS data. Sometimes, an INS sensor has problem with determining the real value of rotation angles in primary measurements epochs. An extended source of data (e.g. GPS observations) must be implemented for the obtained approximate results of rotation angles.

In the paper [4, 10], heading and roll angles were solved using velocity values based on GPS measurements. In this approach, a pitch angle was approximated to 0. The velocity components are derived in the local frame ENU. This technique can be applied while the vehicle speed is over 5 m/s. The accuracy of the presented method depends on the standard deviation of the vehicle velocity.

In the paper [8], the heading course is implemented, using data from a NovAtel OEM4 receiver. Similar like in approaches [4, 10], the heading angle is calculated based on GPS velocities. The standard deviation of the proposed strategy is between  $0.1 \div 0.2$  m/s of the vehicle speed, which corresponds to  $0.6^\circ \div 1^\circ$  of the heading value. The heading information is also applied to correct the INS data.

Two strategies for determination of rotation angles are presented in the paper [3]. In the first approach, rotation angles are estimated from a rotation matrix, using simple trigonometric relations. The least squares estimation is proposed as a mathematical formulation and all results are referenced to the ENU frame in this method. The second technique implements a quaternion operator instead of

the rotation matrix. An extended Kalman filter is utilized in the recursive procedure as a mathematical model. The 6 components of GPS observations are used in computation processing. The mean errors of rotation angles for the first solution are less than  $1^\circ$  and less than  $0.8^\circ$  in the second study.

In this paper, an alternative method for determination of rotation angles is presented. It uses GPS data. Computations were executed in the HPR\_GPS software, whose source code was written in Scilab 5.4.1 editor. Description of HPR\_GPS software with a mathematical model is presented in Section 2. The preliminary results from the HPR\_GPS were very similar to the INS data, but also noisy, which caused that a Kalman filter was used to correct these values. More details about the comparison (e.g. GPS and INS results) can be found in Section 3. The last part of the paper contains some conclusions.

### 2. Mathematical formulation for determination of rotation angles

The HPR\_GPS software is an „open-source” tool, which can be utilized for determination of heading, pitch and roll angles, based on GPS data. The source code of software was written in the Scilab 5.4.1 editor, but it can be executed in version 5.5.0 and also in version 5.3.2. The GPS coordinates in the geodetic frame are basic data in the HPR\_GPS software.

The reference data are saved in a special format in the log file (see Fig. 1). At the first step, the input data with abbreviation „\*.csv” are implemented in the HPR\_GPS tool. Next, the input data are segregated and divided into 7 columns. The column 1 includes a picture number or an epoch number, column 2- latitude, column 3- longitude, column 4- ellipsoidal height, column 5- heading angle, column 6- pitch angle and column 7- roll angle. The geodetic coordinates from 2 to 4 columns are used to obtain the geocentric coordinates ( $X$ ,  $Y$ ,  $Z$ ), based on the Helmert transformation in an iterative process, as follows [7]:

$$e = \sqrt{\frac{a^2 - b^2}{a^2}} \quad (1)$$

$$R = \frac{a}{\sqrt{1 - e^2 \cdot \sin^2 B}} \quad (2)$$

$$X = (R + H) \cdot \cos B \cdot \cos L \quad (3)$$

$$Y = (R + H) \cdot \cos B \cdot \sin L \quad (4)$$

$$Z = (R \cdot (1 - e^2) + H) \cdot \sin B \quad (5)$$

where:  $a, b$  - semi-major and semi-minor axes of the WGS-84 ellipsoid,  $e$  - eccentricity,  $R$  - radius of the curvature of the prime vertical,  $B, L, H$  - geodetic coordinates,  $X, Y, Z$  - geocentric coordinates.

| image        | latitude    | longitude   | altitude | yaw   | pitch | roll  |
|--------------|-------------|-------------|----------|-------|-------|-------|
| DSC09032.JPG | 52.41788338 | 15.13594299 | 278.37   | 89.40 | 4.10  | 0.92  |
| DSC09033.JPG | 52.41788935 | 15.13632049 | 279.08   | 88.94 | 4.09  | 2.28  |
| DSC09034.JPG | 52.41789329 | 15.13663982 | 279.80   | 89.60 | 4.52  | 2.02  |
| DSC09035.JPG | 52.41789408 | 15.13699298 | 279.99   | 91.55 | 2.06  | 1.90  |
| DSC09036.JPG | 52.41789304 | 15.13732730 | 279.32   | 91.16 | 3.63  | 2.11  |
| DSC09037.JPG | 52.41789146 | 15.13759236 | 279.71   | 91.63 | 4.83  | 3.39  |
| DSC09038.JPG | 52.41788132 | 15.13802466 | 280.09   | 92.75 | 3.83  | 1.57  |
| DSC09039.JPG | 52.41787367 | 15.13829267 | 279.98   | 91.81 | 2.82  | -0.23 |
| DSC09040.JPG | 52.41786694 | 15.13863231 | 279.42   | 91.22 | 2.06  | -1.53 |
| DSC09041.JPG | 52.41786685 | 15.13900701 | 278.23   | 90.85 | 2.26  | -0.13 |
| DSC09042.JPG | 52.41786826 | 15.13931599 | 276.86   | 88.19 | 3.51  | 2.13  |
| DSC09043.JPG | 52.41787019 | 15.13969145 | 275.89   | 89.99 | 4.51  | 2.80  |
| DSC09044.JPG | 52.41786812 | 15.13999414 | 275.38   | 89.37 | 6.73  | -1.19 |
| DSC09045.JPG | 52.41786659 | 15.14035856 | 276.22   | 89.99 | 5.97  | 1.31  |
| DSC09046.JPG | 52.41786475 | 15.14071047 | 276.44   | 91.52 | 5.77  | 0.79  |
| DSC09047.JPG | 52.41786258 | 15.14097956 | 276.62   | 90.57 | 5.43  | -2.98 |
| DSC09048.JPG | 52.41786095 | 15.14138413 | 276.80   | 90.44 | 4.94  | 0.39  |
| DSC09049.JPG | 52.41786219 | 15.14166286 | 276.97   | 90.79 | 5.83  | 1.42  |

Fig. 1. The UAV log file with example data

The output geocentric coordinates are used for determination of the aircraft position in the ENU local frame and given by [9]:

$$\Delta e = -\sin L \cdot \Delta X + \cos L \cdot \Delta Y + 0 \cdot \Delta Z \quad (6)$$

$$\Delta n = -\cos L \cdot \sin B \cdot \Delta X - \sin L \cdot \sin B \cdot \Delta Y + \cos L \cdot \Delta Z \quad (7)$$

$$\Delta u = \cos L \cdot \cos B \cdot \Delta X + \sin L \cdot \cos B \cdot \Delta Y + \sin L \cdot \Delta Z \quad (8)$$

where:  $\Delta X, \Delta Y, \Delta Z$  - difference of coordinates for epoch  $t$  and  $t+1$  in the geocentric frame,  $\Delta e, \Delta n, \Delta u$  - difference of coordinates for epoch  $t$  and  $t+1$  in the local frame.

The local coordinates of the aircraft position correspond to the GPS receiver antenna location and differential technique is used for obtaining relative changes of the local coordinates. Moreover, the local coordinates express a baseline vector between epoch  $t$  and  $t+1$ . Finally, the rotation angles (heading  $\psi_{GPS}$ , pitch  $\theta_{GPS}$  and roll  $\phi_{GPS}$ ) are estimated in recursive processing, as below [5]:

$$\Psi_{GPS} = \text{arctg} \left( \frac{\Delta e}{\Delta n} \right) \quad (9)$$

$$\theta_{GPS} = \text{arctg} \left( \frac{\Delta u}{\sqrt{\Delta e^2 + \Delta n^2}} \right) \quad (10)$$

$$\phi_{GPS} = -\text{arctg} \left( \frac{\Delta u}{\Delta e} \right) \quad (11)$$

where:  $\psi_{GPS}, \theta_{GPS}, \phi_{GPS}$  - rotation angles from GPS measurements.

The algorithm of determination of rotation angles in the HPR\_GPS software is realized in recursive processing for  $(n-1)$  steps. The rotation angles are always defined in epoch  $t+1$ , which causes the problem with angles estimated in the first epoch  $t_0$ . For this purpose, in HPR\_GPS software the default value was set to  $0^\circ$ , if the initial value on epoch  $t_0$  was not available. The angles from equations (9-11) had large noise and the Kalman filter method was used for smoothing the rotation angles from the GPS data. The Kalman filter algorithm includes 2 cycles: „Predict”, where equations in this phase are called “Time Update” and

„Correct”, where equations are called “Measurement Update” (see Figure 2).

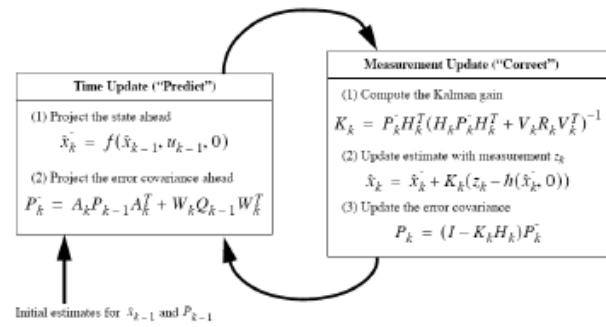


Fig. 2. Flowchart of Kalman filter processing [Kędzierski, 2007]

The first phase of the Kalman filter algorithm expresses a priori value of state ahead and the covariance matrix of rotation angles for a prediction step and it can be described as follows [1, 2]:

- for the heading angle:

$$x_p^h = A \cdot x_{k-1}^h \quad (12)$$

$$P_p^h = A \cdot P_{k-1}^h \cdot A^T + Q_{k-1}^h \quad (13)$$

- for the pitch angle:

$$x_p^p = A \cdot x_{k-1}^p \quad (14)$$

$$P_p^p = A \cdot P_{k-1}^p \cdot A^T + Q_{k-1}^p \quad (15)$$

- for the roll angle:

$$x_p^r = A \cdot x_{k-1}^r \quad (16)$$

$$P_p^r = A \cdot P_{k-1}^r \cdot A^T + Q_{k-1}^r \quad (17)$$

where:  $A$  - matrix of coefficients,  $x_{k-1}^h, x_{k-1}^p, x_{k-1}^r$  - a priori value of the heading, pitch and roll angle from the previous step,  $x_p^h, x_p^p, x_p^r$  - predicted heading, pitch and roll angle,  $P_p^h, P_p^p, P_p^r$  - predicted error of the heading, pitch and roll angle,  $P_{k-1}^h, P_{k-1}^p, P_{k-1}^r$  - a priori covariance matrix for the heading, pitch and roll angle from the previous step,  $Q_{k-1}^h, Q_{k-1}^p, Q_{k-1}^r$  - a priori covariance matrix of process noise for heading, pitch and roll angle from previous step.

The second phase of the Kalman filter algorithm presents a posteriori value for unknown parameters (with covariance errors) and it can be written as below:

- for the heading angle:

$$K_k^h = P_p^h \cdot H_h^T \cdot (H_h \cdot P_p^h \cdot H_h^T + R_h)^{-1} \quad (18)$$

$$x_k^h = x_p^h + K_k^h \cdot (z_h - H_h \cdot x_p^h) \quad (19)$$

$$P_k^h = (I_h - K_k^h \cdot H_h) \cdot P_p^h \quad (20)$$

- for the pitch angle:

$$K_k^p = P_p^p \cdot H_p^T \cdot (H_p \cdot P_p^p \cdot H_p^T + R_p)^{-1} \quad (21)$$

$$x_k^p = x_p^p + K_k^p \cdot (z_p - H_p \cdot x_p^p) \quad (22)$$

$$P_k^p = (I_p - K_k^p \cdot H_p) \cdot P_p^p \quad (23)$$

- for the roll angle:

$$K_k^r = P_p^r \cdot H_r^T \cdot (H_r \cdot P_p^r \cdot H_r^T + R_r)^{-1} \quad (24)$$

$$x_k^r = x_p^r + K_k^r \cdot (z_r - H_r \cdot x_p^r) \quad (25)$$

$$P_k^r = (I_r - K_k^r \cdot H_r) \cdot P_p^r \quad (26)$$

where:  $R_h, R_p, R_r$  - covariance matrix of measurement noise for the heading, pitch and roll angle,  $H_h = H_p = H_r = 1$ ,  $K_k^h = K_k^p = K_k^r$  - gain Kalman matrix for the heading, pitch and roll angle,  $z_h = z_p = z_r$  - vector with measurements for the heading, pitch and roll angle,  $I$  - matrix with 1 along the main diagonal for the heading, pitch and roll angle,  $x_k^h, x_k^p, x_k^r$  - „a posteriori” value for the heading, pitch and roll angle,  $P_k^h, P_k^p, P_k^r$  - „a posteriori” covariance matrix for the heading, pitch and roll angle.

The rotation angles in Kalman filter processing are estimated in an iterative scheme for each measurement epoch. The vector  $T$  with measurements epochs was introduced in computations because the „\*.csv” file did not include any information about the temporal resolution of experiments. The first and last epoch of the vector  $T$  contained numbers 1 and 1472,  $T \in \langle 1; 1472 \rangle$ .

The final results after Kalman filter operation were compared with the raw INS data. The main comparison concerns the determination of the difference of the angles from the GPS and INS measurements and which is given by:

$$d\psi = \sum_1^n \frac{\psi_{INS} - \psi_{GPS}}{n} \quad (27)$$

$$d\theta = \sum_1^n \frac{\theta_{INS} - \theta_{GPS}}{n} \quad (28)$$

$$d\phi = \sum_1^n \frac{\phi_{INS} - \phi_{GPS}}{n} \quad (29)$$

The standard deviations of terms  $(\psi_{INS}, \theta_{INS}, \phi_{INS})$  were also estimated. They are given by:

$$m_{d\psi} = \sqrt{\frac{[v_{d\psi} v_{d\psi}]}{n-1}} \quad (30)$$

$$m_{d\theta} = \sqrt{\frac{[v_{d\theta} v_{d\theta}]}{n-1}} \quad (31)$$

$$m_{d\phi} = \sqrt{\frac{[v_{d\phi} v_{d\phi}]}{n-1}} \quad (32)$$

where:  $\psi_{INS}, \theta_{INS}, \phi_{INS}$  - rotation angles from the INS measurements,  $v_{d\psi} = \psi_{INS} - \psi_{GPS}$ , residuals of the heading angle difference between the GPS and INS data,  $v_{d\theta} = \theta_{INS} - \theta_{GPS}$ , residuals of the pitch angle difference between the GPS and INS data,  $v_{d\phi} = \phi_{INS} - \phi_{GPS}$ , residuals of the roll

angle difference between the GPS and INS data,  $n$  – number of observations,  $n=1472$ .

### 3. Experiment and results

In the studies, the raw data from the log file from a UX5 platform were used. The UX5 platform is mini UAV equipment used in aerial photogrammetry. It can be classified as a mini-sized UAV (Fig. 2.)



Fig. 2. Trimble UX-5 – before flight

The airframe allows fully autonomous flight at the desired height at a preset side-lap and over-lap images coverage. The system includes a flight controller enabling real time flight parameters management. Table 1 presents the basic specifications of the platform.

Tab. 1. Technical parameters of Trimble UX5

| Type         | Body with the wings                                |
|--------------|--|
| Weight       | 2.5 kg   |
| Wing span    | 1 m  |
| Wing surface | 34 dm <sup>2</sup>                                 |
| Dimensions   | 100 × 65 × 10 cm                                   |
| Motor        | Electric motor with propellers (motor power 700 W) |
| Battery      | 14.8 V, 6000 mAh                                   |

The UX5 lets the user control the automatic takeoff, flight and landing. Images are taken using an automatic camera shutter release. Safety of flights is controlled automatically, however, it is possible for the operator to intervene by controlling the emergency safety procedures. The takeoff is possible from the mechanical launcher only.

The system is operable for wind speed not exceeding 18 m/s and in weather conditions no worse than a light rain. The images can be captured from an altitude ranging from 75 to 750 m with a ground resolution from 2.4 to 24 cm. The image data was obtained by a Sony NEX-5R digital camera, which is one of the most commonly selected sensors mounted on board of unmanned aerial vehicles. The captured images are saved in the JPEG format. For the Trimble UX5 platform pictures are taken with a super bright Voigtlander lens with 15 mm focal length and the maximum aperture equal F4.5.

The single-frequency GPS receiver was installed and collected raw data with frequency equal to 10 Hz. The flight time was established to about 45 minutes. The pictures from the flight mission were applied to production of an orthophotomap of the

tested area. The mean value of the flying height was about 272 m, with the maximum and minimum ceiling between 267 and 280 m (see Fig. 3).

The flight was performed in August, 2014 at 10:00 – 11:00 local time over a 1250 m × 3750 m wide area. The trimble UX5 airframe with a SONY NEX5R camera were used to obtain the data. The flight was planned in the *Trimble Aerial Imaging* software.

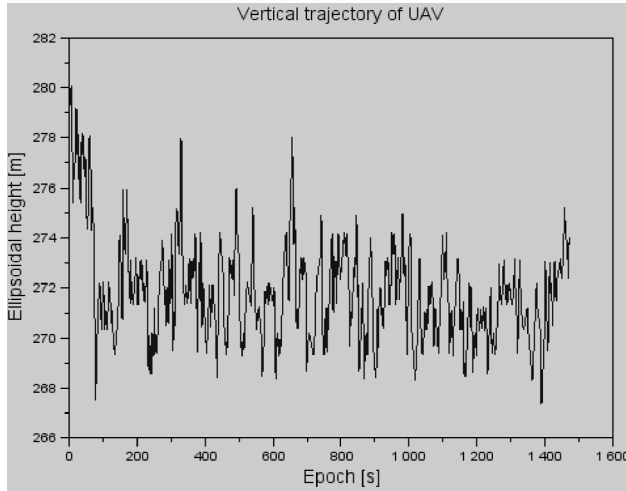


Fig. 3. Vertical trajectory of UAV

Camera preferences were defined manually and the lens focus was set to infinity. The ISO sensitivity was set to AUTO and the aperture was set to 4.5. Due to very poor lighting conditions, the shutter speed had to be set as high as possible, and was fixed at 1/2500 s. In this test, a great number of images were visibly blurred, which further degraded the image radiometric quality. During the first flight 980 images were taken at the altitude of 200 m, with a ground pixel size equal to 0.06 m. Forward and side overlap was equal to 75%. The raids were performed in the East-West direction.

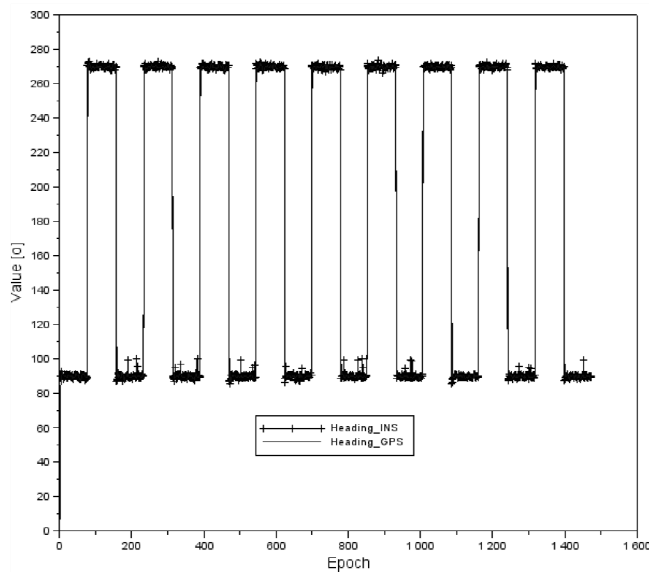


Fig. 4. Value of the heading angle

Figure 4 presents the heading angle for the GPS (from HPR\_GPS software) and INS data. The mean difference  $d\psi$  for the presented values is about  $0.32^\circ$  with the standard deviation of  $5.41^\circ$ . The maximum and minimum values between the GPS and INS data are  $89.40^\circ$  and  $-43.41^\circ$ , respectively. The parameter  $d\psi$  can be treated in this experiment as white noise. Moreover, the

standard deviation  $m_{d\psi}$  is more than  $5^\circ$ , which is less than the boundary error of the heading angle (based on the manual of the UX5 platform, typical errors of rotation angles are close to  $2^\circ$ ). Additionally, blunder errors were eliminated for the heading angle in this experiment by Kalman filter processing. More than 72% results of the difference  $d\psi$  between the GPS and INS sensor are less than  $\pm 1^\circ$ . Whereas, about 95% results of the term  $d\psi$  are less than  $\pm 3^\circ$ .

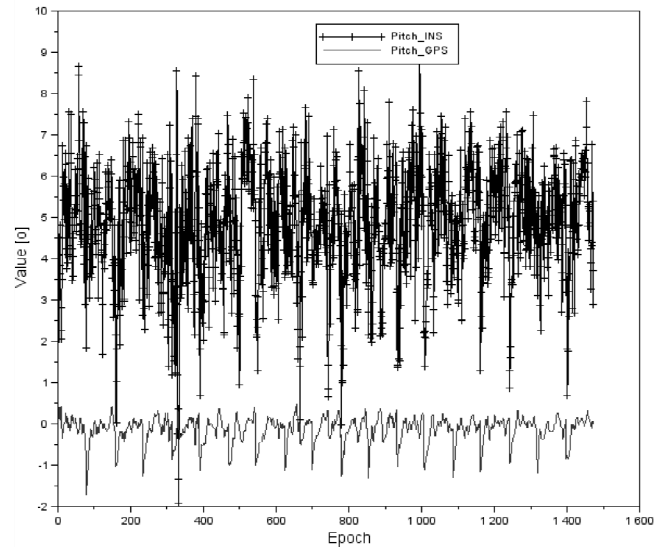


Fig. 5. Value of the pitch angle

Figure 5 shows the pitch angle for the GPS solution and the INS measurements. The mean difference  $d\theta$  for the presented data is about  $4.98^\circ$  with the standard deviation of  $5.06^\circ$ . The maximum and minimum values between the GPS and INS data are  $9.59^\circ$  and  $-2.13^\circ$ , respectively. In reference to the heading and roll angle (based on the INS data), the mean difference  $d\theta$  for the pitch angle has the highest value and the precision of the parameter  $d\theta$  is lower. It should be mentioned that only 49% of the values of the parameter  $d\theta$  are less than  $\pm 5^\circ$ . Additionally, about 95% results of the difference  $d\theta$  are less than  $\pm 7^\circ$ .

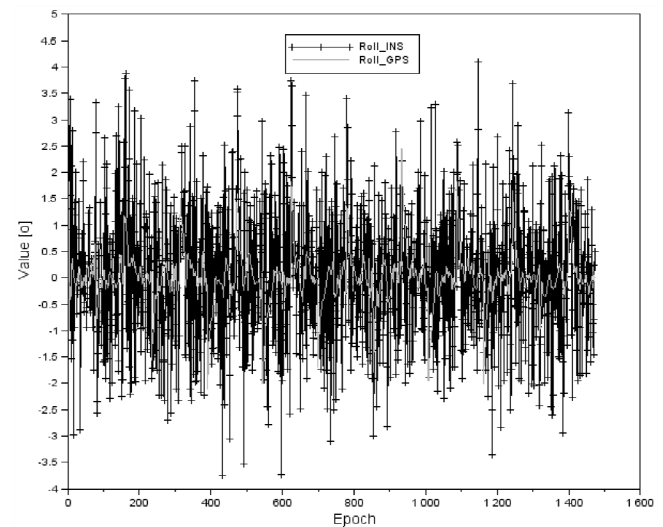


Fig. 6. Value of the roll angle

Figure 6 presents the results of the roll angle for the GPS and INS data. Based on Figure 6, the mean difference  $d\phi$  is about  $0.06^\circ$  with the standard deviation of  $0.69^\circ$ . The magnitude of the results in Fig. 6 is between  $-3.64^\circ$  and  $4.26^\circ$ , adequately. Similarly as for the results of Fig. 4, the parameter  $d\phi$  should be

treated as white noise. The precision and accuracy of the parameter  $d\phi$  is better than that of the heading and pitch angle. The mean errors of the roll angle are smaller with reference to the heading and pitch angles. About 60% results of the difference  $d\phi$  between the GPS and INS sensor are less than  $\pm 1^\circ$ . Moreover, about 99% values of the term  $d\phi$  are less than  $\pm 3^\circ$ .

#### 4. Conclusions

A GPS sensor is very popular in aeronautical navigation. It is applied to obtain an approximate value of rotation angles in many events. Sometimes an INS sensor has problem to obtain values of rotation angles in primary measurement epochs. In this paper, the results of experiment concerning determination of rotation angles using GPS technology are described. The presented research method is based on transformations between the reference geodetic frame and the geocentric frame as well as the local frame of the aircraft. It was assumed that the results of the GPS and INS were analyzed in the same frame. The calculations were executed in the HPR\_GPS software whose source code was written in the Scilab platform. The HPR\_GPS software was characterized and the mathematical model of rotation angle solution was showed. The preliminary results (after Kalman filter operation) show that the standard deviations of the pitch and heading angles are more than  $5^\circ$  and for the roll angle it is less than  $1^\circ$ . The comparison between the GPS and INS sensors shows that the heading and roll angles have white noise trends.

#### 5. References

- [1] Ali A.: Low-Cost Sensors-Based Attitude Estimation for Pedestrian Navigation in GPS-Denied Environments. PhD Thesis, University of Calgary, 2013.
- [2] Cai C.: Precise Point Positioning using dual-frequency GPS and GLONASS measurements. PhD thesis, University of Calgary, 2009.
- [3] Córias J. M. M.: Attitude Determination Using Multiple L1 GPS Receiver. Diploma thesis, Universidade Tecnica de Lisboa, 2012.
- [4] Godha S.: Performance Evaluation of Low Cost MEMS-Based IMU Integrated With GPS for Land Vehicle Navigation Application. Diploma thesis, University of Calgary, 2006.
- [5] Keong J. H.: Determining heading and pitch using a Single Difference GPS/GLONASS approach. Diploma Thesis, University of Calgary, 1999.
- [6] Kędzierski J.: Filtr Kalmana - zastosowania w prostych układach sensorycznych. Koło Naukowe Robotyków Konar, 2007.
- [7] Osada E.: Geodezja. Politechnika Wrocławskiego, Wrocław, 2001.
- [8] Salycheva A. O., Cannon M. E.: Kinematic Azimuth Alignment of INS using GPS Velocity Information, Proceedings of NTM 2004 Conference (Session E3), San Diego, CA, 2004 January 26-28, The Institute of Navigation.
- [9] Sanz Subirana J., Juan Zornoza J. M., Hernández-Pajares M.: GNSS Data Processing. Volume I: Fundamentals and Algorithms, ESA, 2013.
- [10] Shin E. H.: Accuracy Improvement of Low Cost INS/GPS for Land Applications. Diploma thesis, University of Calgary, 2001.
- [11] Yi Y.: On improving the accuracy and reliability of GPS/INS- based direct sensor georeferencing. PhD thesis, The Ohio State University, 2007.

Received: 19.08.2015

Paper reviewed

Accepted: 02.10.2015

Damian WIERZBICKI, PhD, eng.

Alumnus of MUT in Warsaw. His area of interests: UAV photogrammetry, digital image processing.



e-mail: damian.wierzbicki@wat.edu.pl

Kamil KRASUSKI, MSc, eng.

Alumnus of MUT in Warsaw. He is the author of SciTEC Toolbox v.1.0.0 software for determination ionosphere parameters (currently version 1.5.0). His area of interests: navigation, geodesy, physics. Since 2014: Team of Satellites Techniques, since 2015: Faculty of Geodesy, Cartography and Cadastre in District Office in Ryki.



e-mail: kk\_deblin@wp.pl